http://www.uem.br/acta ISSN printed: 1806-2563 ISSN on-line: 1807-8664

Doi: 10.4025/actascitechnol.v35i2.15216

Image analysis for composition monitoring. Commercial blends of olive and soybean oil

Jéssica Kehrig Fernandes¹, Tiemi Umebara¹, Marcelo Kaminski Lenzi^{2*} and Ediely Teixeira da Silva Alves²

¹Programa de Pós-graduação em Engenharia de Alimentos, Universidade Federal do Paraná, Curitiba, Paraná, Brazil. ²Programa de Pós-graduação em Engenharia Química, Universidade Federal do Paraná, Cx. Postal 19011, 81531-980, Curitiba, Paraná, Brazil. *Author for correspondence. E-mail: lenzi@ufpr.br

ABSTRACT. Olive oil represents an important component of a healthy and balanced dietary. Due to commercial features, characterization of pure olive oil and commercial mixtures represents an important challenge. Reported techniques can successfully quantify components in concentrations lower than 1%, but may present long delays, too many purification steps or use expensive equipment. Image analysis represents an important characterization technique for food science and technology. By coupling image and UV-VIS spectroscopy analysis, models with linear dependence on parameters were developed and could successfully describe the mixture concentration in the range of 0-100% in mass of olive oil content. A validation sample, containing 25% in mass of olive oil, not used for parameter estimation, was also used for testing the proposed procedure, leading to a prediction of 24.8 \pm 0.6. Due to image analysis results, 3-parameter-based models considering only R and G components were developed for olive oil content prediction in mixtures with up to 70% in mass of olive oil, the same test sample was used and its concentration was predicted as 24.5 \pm 1.2. These results show that image analysis represents a promising technique for on-line/in-line monitoring of blending process of olive soybean oil for commercial mixtures.

Keywords: edible oils, mixture, sensor, spectroscopy, RGB.

Análise de imagem para monitoramento de composição. Misturas comerciais de azeite de soja e de oliva

RESUMO. O azeite de oliva compõe de dietas saudáveis e balanceadas, assim, sua caracterização é fundamental. Técnicas já reportadas permitem quantificar componentes de misturas em concentrações inferiores a 1%, mas podem apresentar longos atrasos, muitas etapas de purificação prévia e/ou utilizar equipamentos de custo elevado. A análise de imagem representa uma importante técnica de caracterização de alimentos. Usando acoplamento de análise de imagem e espectroscopia UV-VIS, modelos lineares nos parâmetros foram usados para a descrição de misturas de azeite de oliva e óleo de soja no intervalo de concentração de 0-100% de azeite de oliva em massa. Uma amostra com 25% em massa de azeite de oliva foi utilizada para validação da técnica, cuja predição foi de 24,8 ± 0,6. Em função dos resultados da análise de imagem, modelos de três parâmetros considerando apenas as componentes R e G foram desenvolvidos para predição da composição de misturas com até 70% em massa de azeite de oliva. Para a mesma amostra de validação usada, obteve-se uma predição de 24,5 ± 1,2. Assim a análise de imagem é uma técnica promissora e viável para o monitoramento em linha de misturas comerciais de azeite de soja e azeite de oliva.

Palavras-chave: óleos comestíveis, mistura, sensor, espectroscopia, RGB.

Introduction

Olive oil presents growing consumption rates, mainly because its key role played on a balanced and healthy dietary, due to the presence of phenolic antioxidants and their derivatives (FRANKEL, 2011). On the other hand, due to lower costs along with dietary issues, commercial mixtures of olive and other edible oils, usually soybean, are commonly available in local markets. Literature reports different kinds of

olive oil characterization (FRANKEL, 2010), for example, olive oil adulteration either using cheaper vegetable oils or lower grade olive oils; olive oil lipid oxidation and oxidative stability, olive oil volatile compounds, olive oil antioxidants. Consequently, fast and accurate characterization of pure olive oil and commercial mixtures represents an important challenge (GARCIA-GONZALEZ; APARICIO, 2010).

Frequently used analytical techniques for successful oil characterization are based on gas chromatography (PIRAVI-VANAK et al., 2009), high performance liquid chromatography (VEKIARI et al., 2010), nuclear magnetic resonance (ALONSO-SALCES et al., 2010), spectroscopy (SILVEIRA et al., 2010), electronic (MILDNER-SZKUDLARZ; JELEN, 2010), thermophysical properties analysis (TORRECILLA et al., 2011), among others. Regarding olive oil adulteration, these techniques are reported to quantify contaminants in concentrations ranging from 1 to 5% in mass content; however, some may identify even lower amounts.

Image analysis represents an important characterization technique (RIBEIRO; CENTENO, 2009) for food science and technology (ZHENG et al., 2006). Due to noninvasive and precision/accuracy features, a broad range of applications became feasible (LIU et al., 2011). The use of image analysis for olive oil processing and characterization is still insipient. Ram et al. (2010) used image analysis in order to optimize the harvest time, by correlating olive color characteristics to oil content and quality. Gordillo et al. (2011) evaluated the influence of turbidity grade on color and appearance of virgin olive oil, however, their work focused on filtered and non-filtered olive oil. Therefore, image analysis remains as an important alternative tool for future developments on olive oil mixture characterization. It is important to stress that image analysis may be useful not only for soybean and olive oil mixtures, but it may also be useful for characterization of mixtures with different edible oils as long as a color change occurs.

According to Marchal et al. (2011), the lack of proper instrumentation providing fast and reliable information for process control still remains a challenge in olive oil processing, in order to avoid performing the standard laboratory analysis. Therefore, this manuscript reports the development of a simple and low cost approach to olive and soybean oil mixtures characterization, which can be used for process instrumentation, focusing, for example, on olive oil mixtures monitoring. More specifically, image analysis and image analysis coupled with UV-VIS spectra were used for model formulation in order to predict mixture contents by proper parameter estimation.

Material and methods

Material

Extra virgin olive oil (La Violetera, free acid content less than 0.4%) and soybean oil (COCAMAR, Brazil) purchased at local market were used as received without further purification. Table 1 presents the composition (in olive oil mass percent) of the prepared mixtures used for obtaining experimental data. Also a test mixture of 25% of olive oil was also analyzed for model validation purposes. Samples were weighted in an analytical scale (BioPrecisa, model: FA 2104N, Precision: 0.0001 g).

Methods – image analysis

After weighting, each sample was transferred to a polystyrene cuvette (Kartell S.P.A., Italy) with 0.1 m of light path and 4.5·10⁻³ L of capacity. All samples were placed, side-by-side, inside a chamber with a light source in order to minimize environmental interference and provide the same thickness of fluid for all samples, as the thicker sample; the darker it seems to be. Afterwards, photographs of the samples were taken using a Sony Cyber-Shot Machine (7.2 Mega pixels). Camera zoom was fixed at 1x and it was placed 25 cm away from the chamber in order to frame all cuvettes in a single photograph.

Image analysis was processed by multi-task software (SILVA; LENZI, 2011). RGB (Red-Green-Blue) color system (GONZALEZ; WOODS, 2007) was used for sample image characterization. For each sample, rectangles containing over 10000 pixels were selected for color decomposition in components R, G, B. This number of pixels is high enough to assure robustness to the image analysis procedure and guarantee low mean confidence interval bands for each color component of each sample.

Methods – UV-VIS analysis

Immediately after taking photographs, each sample was analyzed by a UV-VIS spectrophotometer (Cary 100 Scan UV-Visible Spectrophotometer – Agilent Technologies). Samples were scanned in the range of 190 to 900 nm of wavelength and absorbance was recorded. Values of absorbance in different wavelengths (374, 416, 427, 455, 460, 483 and 670 nm) were selected for further analysis.

Table 1. Mixtures composition used for characterization (in olive oil mass percent).

M0	M10	M20	M30	M40	M50	M60	M70	M80	M90	M100
0	10	20	30	40	50	60	70	80	90	100

Methods – parameter estimation

In order to quantify the oil mixture composition, olive oil mass percent was correlated to the mean value of R, G, and B components of the image analysis and to the absorbance in the previously selected peaks and valleys. Models with linear dependence on parameters were used to fit the experimental data of olive oil mass percent, considering minimum least squares as objective function. Parameter estimation performed using Levenberg-Marquadt algorithm (LEVENBERG, 1944; MARQUARDT, 1963). The numerical parameter estimation problem had 10⁻⁶ as convergence criteria. Model validation tests and parameter variance and covariance calculations were performed using the procedure adopted by Isfer et al. (2010). Due to the linear feature of parameter estimation problem, a unique value of 1.0 was used as initial parameter guess.

The first case studied comprised the mixture composition prediction along the full range of 0 to 100% in mass of olive oil, while a second study case, along the concentration range of 0 to 70% was also carried out. Models with 2, 3, 4, 5, 6, 7 parameters where fitted. Models containing 8 or more parameters were not considered in order to avoid possible experimental error fitting.

Finally, it is worth mentioning that the test sample, containing 25% in mass of olive oil, was not used for parameter estimation, it was only used for model validation. The model validation not only comprises the model prediction but also the standard deviation of its prediction. In this sense, only parameter variance and covariance (PINTO, 1998) were considered, consequently, the standard error of the model prediction is given by Equation 1:

$$s_{mass} = \sqrt{\sum_{i=1}^{NP} \left(\frac{\partial mass}{\partial ai}\right)^2 \cdot s_{ai}^2 + 2 \cdot \sum_{i=1}^{NP-1} \sum_{j=i+1}^{NP} \left(\frac{\partial mass}{\partial ai}\right) \cdot \left(\frac{\partial mass}{\partial aj}\right) \cdot s_{ai-aj}^2} \qquad \left(1\right)$$

where:

NP is the number of parameters;

 s_{ai}^2 is the parameter ai variance;

 s_{ai-aj}^2 is the covariance of parameters ai and aj.

Results and discussion

Sample characterization

Figure 1 presents some of the oil samples used in this work. It is interesting to note the presence of a color gradient, where the samples become darker by increasing the amount of olive oil.

Image analysis results are summarized by Table 2, which presents basic descriptive statistics of component R, G and B of each sample. It must be emphasized that

maximum range of variation of R, G, B values goes from 0 to 255. On the other hand, Figure 2 compares the behavior of the three color components according to an increase in the olive oil content.

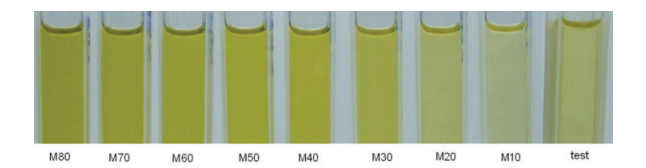


Figure 1. Oil samples (M80 to M10 and test sample).

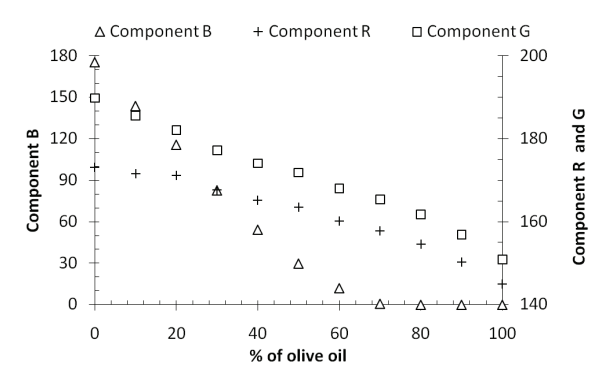


Figure 2. R, G, B behavior with olive oil percent variation.

It can be seen that components R and G continuously change along the concentration range. This behavior, however, is not observed for component B, which continuously changes up to roughly 70% mass content of olive oil in the mixture. On the other hand, the range of values of component B is much larger than the other components. It can be seen that the standard error of the means is roughly constant, indicating a robust method. Finally, kurtosis and skewness indicate that the collected data can be considered normally distributed over the mean, thus allowing the conclusion that the means are not biased and deviations occur due to random errors.

Figure 3 presents the obtained raw spectra in the range of 350 to 700 nm. It is important to stress that the raw spectra were directly used for modeling purposes. More specifically, absorbance in three valleys (374, 427 and 460 nm) and four peaks (416, 455, 483 and 670 nm) were selected for mixtures characterization. These wavelengths were selected because they presented the higher absorbance variance, allowing a better discrimination of the mass content. It must be stressed that this procedure (using raw spectra and samples with no purification) was adopted in order to develop a robust characterization method. The absorbance in each wavelength selected for modeling purposes is shown in Table 3.

Table 2. Summary of R, G, B color components for each sample.

Component	Mean	Lower Quartile	Upper Quartile	Standard Error of Mean	Skewness	Kurtosis
R_M0	173.034	172	174	0.018	0.21	0.29
R_M10	171.518	170	173	0.018	0.13	-0.077
R_M20	171.189	170	173	0.018	-0.28	0.25
R_M30	167.663	166	169	0.017	0.093	0.62
R_M40	165.127	163	167	0.024	-0.053	2.6
R_M50	163.507	162	165	0.019	-0.099	0.16
R_M60	160.172	159	162	0.019	-0.12	0.023
R_M70	157.809	157	159	0.016	-0.12	0.31
R_M80	154.520	154	156	0.014	-0.18	1.8
R_M90	150.198	149	152	0.019	-0.28	0.81
R_M100	144.975	143	147	0.022	-0.12	0.16
G_M0	189.795	189	191	0.017	0.19	0.15
G_M10	185.596	185	187	0.015	-0.045	0.32
G_M20	182.069	181	183	0.015	0.078	0.45
G_M30	177.214	176	178	0.014	-0.089	0.98
G_M40	174.07	172	176	0.024	-0.093	2.21
G M50	171.863	170	173	0.018	0.078	-0.29
G_M60	167.995	167	169	0.016	-0.0024	0.36
G M70	165.346	164	166	0.015	0.14	0.15
G M80	161.722	161	163	0.015	-0.083	1.53
G_M90	156.918	156	158	0.018	-0.28	0.69
G_M100	150.876	149	152	0.022	-0.20	0.36
B M0	175.515	174	177	0.019	0.17	-0.034
B_M10	143.857	143	145	0.017	0.41	0.69
B M20	115.815	114	117	0.018	0.26	0.29
B_M30	82.7516	81	85	0.025	0.34	-0.18
B_M40	54.359	51	57	0.041	0.72	0.52
B_M50	29.859	28	31	0.021	0.057	0.099
B_M60	12.059	11	13	0.017	0.011	0.42
B_M70	0.776	0	1	0.010	1.7	3.3
B M80	0	0	0	0	-	-
B_M90	0	0	0	0	-	-
B M100	0	0	0	0	_	-

Table 3. Absorbance values.

MIXTURE	ABS374	ABS416	ABS427	ABS455	ABS460	ABS483	ABS670
M0	0.5067	0.2844	0.2025	0.09732	0.08701	0.06492	0.06496
M10	0.6949	0.5486	0.4106	0.2669	0.2480	0.1972	0.1194
M20	0.7555	0.7444	0.5764	0.4347	0.4088	0.3382	0.1809
M30	0.7362	0.8454	0.6747	0.5626	0.5324	0.4553	0.2378
M40	0.8364	1.067	0.8624	0.7460	0.7081	0.6099	0.3092
M50	0.9549	1.349	1.099	0.9789	0.9300	0.8041	0.3942
M60	1.003	1.455	1.191	1.070	1.017	0.8814	0.4291
M70	1.094	1.700	1.399	1.277	1.215	1.055	0.5052
M80	1.196	1.927	1.599	1.473	1.402	1.220	0.5780
M90	1.278	2.111	1.765	1.640	1.560	1.362	0.6418
M100	1.370	2.302	1.944	1.821	1.734	1.517	0.7117

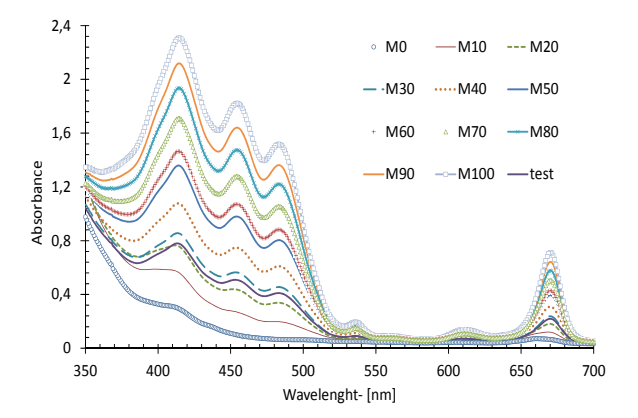


Figure 3. UV-VIS Spectra.

Results for olive oil concentration range 0-100%

In this study, the models were divided into classes according to the number of parameters, more precisely, 2, 3, 4, 5, 6, 7. The best model of each class is shown in Table 4. By best model, it is meant a model that resulted in the lowest objective function value within each class of models, as well as presented all parameters with higher values than the correspondent parameter standard deviation. As expected, the higher the number of parameters, the lower the value of the objective function, the better the predictions are expected to be. This can be observed in Figure 4, where model residues (experimental – model prediction) are plotted against experimental values of olive oil content.

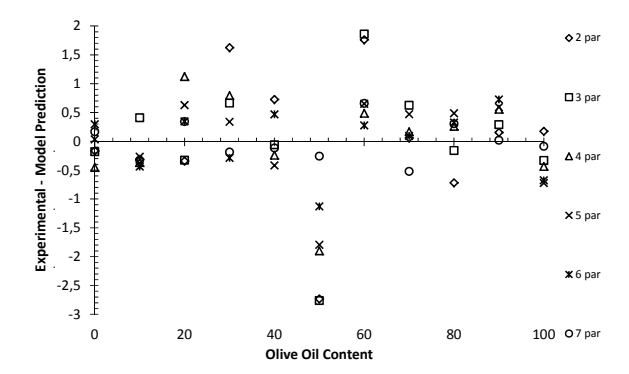


Figure 4. Residual values of model predictions – 0-100% of olive oil.

As mentioned, the test sample containing 25% of mass of olive oil was also characterized for model

validation purposes and it was not considered for model parameter estimation. Table 5 presents the results of this sample characterization, used for further model predictions.

By substituting these values in the models presented in Table 5 and using Equation 1, one can calculate model predictions and the correspondent standard deviation as shown in Figure 5. The model with 3 parameters presents the best prediction not only considering in the composition itself, but also its standard deviation. It is important to stress that this model includes R, G and ABS670, consequently it indicates that the coupled use of image analysis and UV-VIS spectra improves the composition prediction.

Table 4. Summary of models – concentration range 0-100% in mass of olive oil

Parameters	Model								
		$mass = a0 \cdot B + a1 \cdot ABS460$							
	Objective Function: 14.5	R =0	.999						
	Parameters	Parameter C	Covariance						
	$a0 = (-27.6 \pm 4.8) \cdot 10^{-3}$	(a0-a1) = -	4.25.10-4						
	$a1 = (+575.9 \pm 3.8) \cdot 10^{-1}$		- 4.23-10						
		$ass = a0 \cdot R + a1 \cdot G + a2 \cdot ABS670$							
	Objective Function: 12.5	R =0							
	Parameters	Parameter C							
	$a0 = (+5.6 \pm 2.8) \cdot 10^{-1}$	$(a0-a1) = -7.13 \cdot 10^{-2}$							
	$a1 = (-5.6 \pm 2.6) \cdot 10^{-1}$	$(a0-a2) = -7.37 \cdot 10^{-1}$							
	$a2 = (+ 145.6 \pm 3.1) \cdot 10^{0}$	(a1-a2) = +	- 6.75·10 ⁻¹						
		$= a0 + a1 \cdot R + a2 \cdot B + a3 \cdot ABS455$							
	Objective Function: 6.7	R =0							
	Parameters	Parameter C	Covariance						
	$a0 = (+ 16.4 \pm 5.8) \cdot 10^{+1}$	$(a0-a1) = -1.79 \cdot 10^{+1}$	$(a1-a2) = +5.10 \cdot 10^{-3}$						
	$a1 = (-8.8 \pm 3.1) \cdot 10^{-1}$	(a0-a1) = -1.7710 $(a0-a2) = -9.64 \cdot 10^{-1}$	$(a1-a2) = +3.16 \cdot 10$ $(a1-a3) = +2.07 \cdot 10^0$						
	$a2 = (-8.2 \pm 2.1) \cdot 10^{-2}$	$(a0-a2) = -3.85 \cdot 10^{+2}$ $(a0-a3) = -3.85 \cdot 10^{+2}$	$(a2-a3) = +1.27 \cdot 10^{-1}$						
	$a3 = (+35.4 \pm 6.8) \cdot 10^{0}$, ,	(42 46) 11.2, 10						
		$0 + a1 \cdot R + a2 \cdot G + a3 \cdot B + a4 \cdot ABS455$	000						
	Objective Function: 5.7	R = 0							
	Parameters	Parameter C							
	$a0 = (+17.2 \pm 5.8) \cdot 10^{+1}$	$(a0-a1) = -1.55 \cdot 10^{+1}$	$(a1-a3) = +1.01 \cdot 10^{-2}$						
	$a1 = (-5.5 \pm 4.6) \cdot 10^{-1}$	$(a0-a2) = -2.56 \cdot 10^{0}$	$(a1-a4) = +1.86 \cdot 10^{\circ}$						
	$a2 = (-3.6 \pm 3.4) \cdot 10^{-1}$	$(a0-a3) = -8.42 \cdot 10^{-1}$	$(a2-a3) = -5.50 \cdot 10^{-3}$						
	$a3 = (-6.6 \pm 2.6) \cdot 10^{-2}$	$(a0-a4) = -3.87 \cdot 10^{+1}$	$(a2-a4) = +2.08 \cdot 10^{-1}$						
	$a4 = (+34.7 \pm 6.8) \cdot 10^{0}$	$(a1-a2) = -1.12 \cdot 10^{-1}$	$(a3-a4) = + 1.17 \cdot 10^{-1}$						
		+ a2·B + a3·ABS416 + a4·ABS455 + a5·ABS6 R = 0							
	Objective Function: 3.2 Parameters	Parameter C							
	Parameters	$(a0-a1) = -2.32 \cdot 10^{+1}$	Covariance						
	$a0 = (+28.5 \pm 7.1) \cdot 10^{+1}$	$(a0-a1) = -2.52 \cdot 10$ $(a0-a2) = -1.90 \cdot 10^{0}$	$(a1-a5) = + 3.54 \cdot 10^{+1}$						
	` ,	$(a0-a2) = -1.90^{\circ}10$ $(a0-a3) = -1.41^{\circ}10^{+3}$	$(a2-a3) = + 1.07 \cdot 10^{0}$						
	$a1 = (-13.2 \pm 3.4) \cdot 10^{-1}$		$(a2-a4) = -3.91 \cdot 10^{0}$						
	$a2 = (-14.3 \pm 3.1) \cdot 10^{-2}$	$(a0-a4) = +5.85 \cdot 10^{+3}$	$(a2-a5) = + 7.67 \cdot 10^{0}$						
	$a3 = (-8.9 \pm 4.9) \cdot 10^{+1}$ $a4 = (+3.8 \pm 1.7) \cdot 10^{+2}$	$(a0-a5) = -1.27 \cdot 10^{+4}$ $(a1-a2) = +7.60 \cdot 10^{-3}$	$(a3-a4) = -8.15 \cdot 10^{+3}$						
	$a4 = (+3.8 \pm 1.7)^{10}$ $a5 = (-6.8 \pm 3.0) \cdot 10^{+2}$	$(a1-a2) = +7.00 \cdot 10$ $(a1-a3) = +2.17 \cdot 10^{0}$	$(a3-a5) = + 1.44 \cdot 10^{+4}$						
	$a3 = (-0.8 \pm 5.0)^{-10}$	(a1-a3) = +2.1740 $(a1-a4) = -1.33 \cdot 10^{+1}$	$(a4-a5) = -5.07 \cdot 10^{+4}$						
	$mass = 20 + 21 \cdot R + 27$	2·B + a3·G + a4·ABS374 + a5·ABS427 + a6·Al	R\$460						
	Objective Function: 1.17	R = 0							
	Parameters	Parameter C							
		$(a0-a1) = -2.59 \cdot 10^{+1}$							
		$(a0-a2) = +3.49 \cdot 10^{-1}$	$(a2-a3) = -2.40 \cdot 10^{-3}$						
	$a0 = (+42.6 \pm 7.2) \cdot 10^{+1}$	$(a0-a2) = 1.06 \cdot 10^{0}$	$(a2-a4) = -6.85 \cdot 10^{-2}$						
	$a0 = (142.0 \pm 7.2) \cdot 10^{0}$ $a1 = (-18.2 \pm 4.2) \cdot 10^{0}$	$(a0-a4) = -3.89 \cdot 10^{+3}$	$(a2-a5) = + 1.34 \cdot 10^{0}$						
	$a2 = (-3.1 \pm 2.0) \cdot 10^{-2}$	$(a0-a5) = +1.13\cdot10^{+4}$	$(a2-a6) = -1.47 \cdot 10^{0}$						
	$a2 = (-3.1 \pm 2.0)^{-10}$ $a3 = (-10.8 \pm 2.0) \cdot 10^{-3}$	$(a0-a5) = +1.15\cdot10$ $(a0-a6) = -1.05\cdot10^{+4}$	$(a3-a4) = +5.83 \cdot 10^{-1}$						
	$a3 = (-10.8 \pm 2.0)^{110}$ $a4 = (-24.6 \pm 6.3) \cdot 10^{+1}$	$(a0-a0) = -1.03 \cdot 10$ $(a1-a2) = -4.53 \cdot 10^{-2}$	$(a3-a5) = -1.84 \cdot 10^{\circ}$						
	$a4 = (-24.6 \pm 0.5)^{110}$ $a5 = (+7.1 \pm 1.8) \cdot 10^{+2}$	$(a1-a2) = -4.53^{\circ}10$ $(a1-a3) = +7.60 \cdot 10^{-3}$	$(a3-a6) = + 1.76 \cdot 10^0$						
	$a6 = (+7.1 \pm 1.8)^{4}10^{4}$ $a6 = (-6.1 \pm 1.6) \cdot 10^{+2}$		$(a4-a5) = -1.11 \cdot 10^{+4}$						
	au = (= 0.1 ± 1.0)·10	$(a1-a4) = +1.84 \cdot 10^{+1}$	$(a4-a6) = + 1.01 \cdot 10^{+4}$						
		$(a1-a5) = -5.52 \cdot 10^{+1}$ $(a1-a6) = +5.15 \cdot 10^{+1}$	$(a5-a6) = -2.89 \cdot 10^{+4}$						

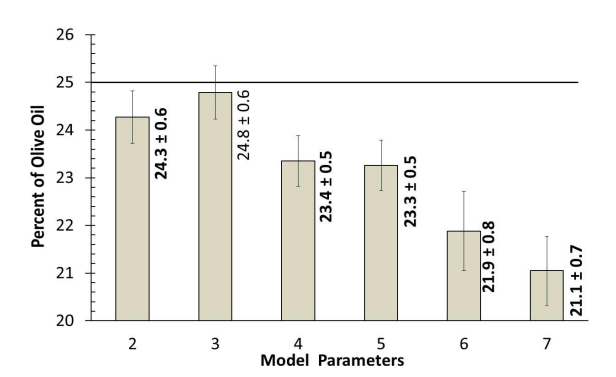


Figure 5. Model predictions (0-100%).

Due to the lower values of the objective function, one might expect that the larger the number of parameters, the better the model prediction. This is true for predictions close enough to the used experimental data, as one can see in Figure 4, in which the residuals of the model with 7 parameters are much closer to 0 when compared to the residuals of the other models.

On the other hand, the number of parameters considerably interfere in the model behavior in between the data used for estimation, therefore, a larger number of parameters may reduce the model likelihood, yielding poorer predictions, which was the case analyzed here, as the test sample (25% of olive oil) lies in between to samples used for parameter estimation (20 and 30% of olive oil). This probably happens because models with a larger number of parameters may fit experimental error and not the data behavior itself. This leads to an optimum number of parameters, which in our study is 3.

Finally, it is important to highlight that this technique can be considered as an alternative for

on-line/in-line sensor development focusing on commercial olive oil mixture concentration monitoring in the range of 0-100% of olive content. For process implementation, model improvement can be simply achieved by considering more samples for parameter estimation, for example, instead of an interval o 10%, an interval of 5% in olive oil content could have been chosen.

Results for olive oil concentration range 0-70%

Commercial mixtures of olive oil with contents up to 70% can be usually found in local markets. Consequently, prediction models for this range of concentration were also obtained, nevertheless, considering correlation only to image analysis results. Based on the results of Figure 5, models with 3 parameters and only based on R and G components were tested. Table 6 presents the parameter estimation results.

The residuals of these models were also evaluated and are presented in Figure 6. For sake of comparison, the residuals of the model with three parameters reported in Table 5 (3 par (0-100%)) were also plotted, however, it must be noted that this model was estimated for the full concentration range and also uses UV-VIS absorbance data. One can observe that for the range of 0-70% the residuals of all models reported in Table 6 remain in the same range. It can be seen that image analysis components R and G can be used for successful olive oil content monitoring. For example, for quantities of 10; 50; 60; 70%, models reported in Table 6, which use only image analysis, presents results as accurate as the best model obtained for the range of 0-100% of olive oil composition.

Table 5. Sample test characterization – 25% mass of olive oil.

R	G	В	ABS374	ABS416	ABS427	ABS455	ABS460	ABS483	ABS670
168.639	181.418	119.586	0.7030	0.7692	0.6142	0.5063	0.4789	0.4099	0.2189

Table 6. Summary of models – concentration range 0-70% in mass of olive oil.

Parameters	M	lodel		
	mass = a0 -	+ a1·R + a2·G		
	Objective Function: 16.9	R = 0.998		
M. 1.14	Parameters	Parameter Covariance		
Model 1	$a0 = (+61.2 \pm 3.7) \cdot 10^{+1}$	$(a0-a1) = -2.21\cdot10^{+1}$		
	$a1 = (-13.8 \pm 6.4) \cdot 10^{-1}$	$(a0-a2) = + 1.29 \cdot 10^{+1}$		
	$a2 = (-19.6 \pm 4.2) \cdot 10^{-1}$	$(a1-a2) = -2.63 \cdot 10^{-1}$		
	$mass = a0 \cdot R^2 +$	+ a1·G + a2 R ² G		
	Objective Function: 28.9	R = 0.997		
Model 2	Parameters	Parameter Covariance		
Wiodel 2	$a0 = (+ 9.5 \pm 3.4) \cdot 10^{-3}$	$(a0-a1) = -1.32 \cdot 10^{-3}$		
	$a1 = (+13.5 \pm 3.9) \cdot 10^{-1}$	$(a0-a2) = + 1.87 \cdot 10^{-8}$		
	$a2 = (-95.3 \pm 6.2) \cdot 10^{-6}$	$(a1-a2) = + 1.88 \cdot 10^{-6}$		
	$mass = a0 \cdot R^2 +$	$a1 \cdot R \cdot G + a2 R^2 G$		
	Objective Function: 32.1	R = 0.996		
Model 3	Parameters	Parameter Covariance		
Model 3	$a0 = (+ 9.2 \pm 3.8) \cdot 10^{-3}$	$(a0-a1) = -1.94 \cdot 10^{-5}$		
	$a1 = (+ 16.7 \pm 5.2) \cdot 10^{-3}$	$(a0-a2) = +3.57 \cdot 10^{-8}$		
	$a2 = (-14.5 \pm 1.1) \cdot 10^{-5}$	$(a1-a2) = -5.44 \cdot 10^{-8}$		

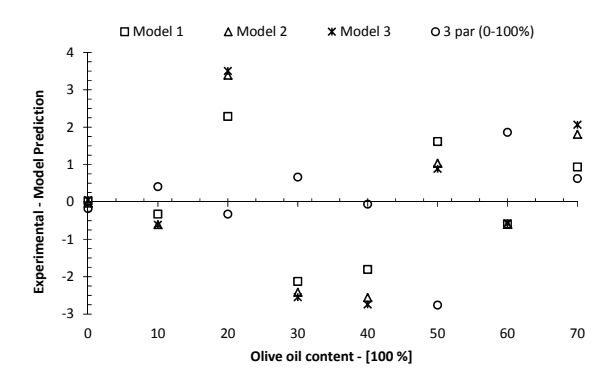


Figure 6. Residual values of model predictions – 0-70% of olive

Figure 7 shows the model predictions and the correspondent standard deviation for the test sample. It can be seen that predictions of the models listed in Table 6 are close to the target value, however, different model configurations may improve the obtained results. As mentioned before model improvement can also be achieved by considering more samples for parameter estimation, for example, instead of an interval o 10%, an interval of 5% in olive oil content could have been chosen. Consequently, R, G components can be successfully used for olive and soybean oil mixture composition monitoring. Finally, it is worth emphasizing that predictions using only image analysis components can be regarded as accurate as the predictions using UV-VIS spectra, allowing the development of a fast low cost sensor.

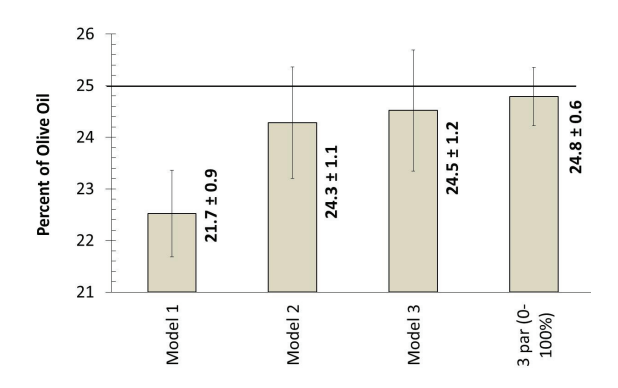


Figure 7. Model predictions (0-70%).

Conclusion

A simple and low cost technique was proposed for olive and soybean oil mixture composition prediction. By coupling image and UV-VIS spectroscopy analysis, models with linear dependence on parameters were developed and successfully could describe the mixture concentration in the range of 0-100% in mass of olive oil content. More specifically, models with 2,

3, 4, 5, 6 and 7 parameters were used. A validation sample, containing 25% in mass of olive oil was also used for testing the proposed procedure. All models could predict the olive oil content in the sample, however, according to the results, the model with 3 parameters provided the best performance and prediction error. Due to image analysis results, 3parameters-based models considering only R and G components were developed for olive oil content prediction in mixtures with up to 70% in mass of olive oil. The test sample was also used for validation purposes, leading to good predictions. These results show that image analysis represents a promising technique for on-line/in-line monitoring of blending process of olive soybean oil for commercial mixtures.

Acknowledgements

The authors thank Fundação Araucária, CNPq and CAPES (Brazilian Agencies) for financial support of this work and Ana Paula Pitarello for useful discussions regarding UV-VIS analysis.

References

ALONSO-SALCES, R. M.; HEBERGER, K.; HOLLAND, M. V.; MORENO-ROJAS, J. M.; MARIANI, C.; BELLAN, G.; RENIERO, F.; GUILLOU, C. Multivariate analysis of NMR fingerprint of the unsaponifiable fraction of olive oils for authentication purposes. **Food Chemistry**, v. 118, n. 4, p. 956-965, 2010.

FRANKEL, E. N. Chemistry of extra virgin olive oil: adulteration, oxidative stability, and antioxidants. **Journal of Agricultural and Food Chemistry**, v. 58, n. 10, p. 5991-6006, 2010.

FRANKEL, E. N. Nutritional and biological properties of extra virgin olive oil. **Journal of Agricultural and Food Chemistry**, v. 59, n. 3, p. 785-792, 2011.

GARCIA-GONZALEZ, D. L.; APARICIO, R. Research in olive oil: challenges for the near future. **Journal of Agricultural and Food Chemistry**, v. 58, n. 24, p. 12569-12577, 2010.

GONZALEZ, R. C.; WOODS, R. E. **Digital Image Processing**. Upper Saddle River: Prentice Hall, 2007.

GORDILLO, B.; CIACCHERI, L.; MIGNANI, A. G.; GONZALEZ-MIRET, M. L.; HEREDIA, F. J. Influence of turbidity grade on color and appearance of virgin olive oil. **Journal of the American Oil Chemists Society**, v. 88, n. 9, p. 1317-1327, 2011.

ISFER, L. A. D.; LENZI, M. K.; LENZI, E. K. Identification of biochemical reactors using fractional differential equations. **Latin American Applied Research**, v. 40, n. 2, p. 193-198, 2010.

LEVENBERG, K. A method for the solution of certain problems in least squares. **Quarterly Applied Mathematics**, v. 2, n. 2, p. 164-168, 1944.

LIU, J.; YANG, W. W.; WANG, Y. S.; RABABAH, T. M.; WALKER, L. T. Optimizing machine vision based applications in agricultural products by artificial neural network. **International Journal of Food Engineering**, v. 7, n. 3, 2011.

MARCHAL, P. C.; ORTEGA, J. G.; PUERTO, D. A.; GARCIA, J. Current situation and future perspectives on virgin olive oil elaboration process control. **Revista Iberoamericana de Automatica e Instrumentacion**, v. 8, n. 3, p. 258-269, 2011.

MARQUARDT, D. An algorithm for least-squares estimation of nonlinear parameters. **SIAM Journal of Applied Mathematics**, v. 11, n. 2, p. 431-441, 1963.

MILDNER-SZKUDLARZ, S.; JELEN, H. H. Detection of olive oil adulteration with rapeseed and sunflower oils using MOS electronic nose and SMPE-MS. **Journal of Food Quality**, v. 33, n. 1, p. 21-41, 2010.

PINTO, J. C. On the costs of parameter uncertainties. Effects of parameter uncertainties during optimization and design of experiments. **Chemical Engineering Science**, v. 53, n. 11, p. 2029-2040, 1998.

PIRAVI-VANAK, Z.; GHAVAMI, M.; EZZATPANAH, H.; ARAB, J.; SAFAFAR, H.; GHASEMI, J. B. Evaluation of authenticity of iranian olive oil by fatty acid and triacylglycerol profiles. **Journal of the American Oil Chemists Society**, v. 86, n. 9, p. 827-833, 2009.

RAM, T.; WIESMAN, Z.; PARMET, I.; EDAN, Y. Olive oil content prediction models based on image processing. **Biosystems Engineering**, v. 105, n. 2, p. 221-232, 2010.

RIBEIRO, S. R. A.; CENTENO, J. A. S. A simplified merging method applied to image data for purposes of visual interpretation. **Acta Scientiarum**. **Technology**, v. 31, n. 1, p. 1-7, 2009.

SILVA, E. T. A.; LENZI, M. K. Development of a didactic module for real-time level control based on image analysis. Canadian Journal on Image Processing and Computer Vision, v. 2, n. 5, p. 46-48, 2011.

SILVEIRA, F. L.; SILVEIRA, L.; VILLAVERDE, A. B.; PACHECO, M. T. T.; PASQUALUCCI, C. A. Use of dispersive Raman spectroscopy in the determination of unsaturated fat in commercial edible oil- and fatcontaining industrialized foods. **Instrumentation Science and Technology**, v. 38, n. 1, p. 107-123, 2010.

TORRECILLA, J. S.; GARCIA, J.; GARCIA, S.; RODRIGUEZ, F. Quantification of adulterant agents in extra virgin olive oil by models based on its thermophysical properties. **Journal of Food Engineering**, v. 103, n. 2, p. 211-218, 2011.

VEKIARI, S. A.; OREOPOULOU, V.; KOURKOUTAS, Y.; KAMOUN, N.; MSALLEM, M.; PSIMOULI, V.; ARAPOGLOU, D. Characterization and seasonal variation of the quality of virgin olive oil of the throumbolia and koroneiki varieties from southern Greece. **Grasas y Aceites**, v. 61, n. 3, p. 221-231, 2010.

ZHENG, C. X.; SUN, D. W.; ZHENG, L. Y. Recent applications of image texture for evaluation of food qualities - A review. **Trends in Food Science and Technology**, v. 17, n. 3, p. 113-128, 2006.

Received on November 7, 2011. Accepted on January 20, 2012.

License information: This is an open-access article distributed under the terms of the Creative Commons Attribution License, which permits unrestricted use, distribution, and reproduction in any medium, provided the original work is properly cited.